2010-06

Molecular-level interactions of an azopolymer and poly(dodecylmethacrylate) in mixed Langmuir and Langmuir-Blodgett films for optical storage

Journal of Colloid and Interface Science,Maryland Heights : Academic Press,v. 346, n. 1, p. 87-95, June 2010
http://www.producao.usp.br/handle/BDPI/50165

Journal of Colloid and Interface Science 346 (2010) 87–95

Contents lists available at ScienceDirect

Journal of Colloid and Interface Science

www.elsevier.com/locate/jcis

Molecular-level interactions of an azopolymer and poly(dodecylmethacrylate) in mixed Langmuir and Langmuir–Blodgett films for optical storage

Lucinéia F. Ceridório [a], Débora T. Balogh [a], Luciano Caseli [b], Marcos R. Cardoso [a], Tapani Viitala [c], Cleber R. Mendonça [a], Osvaldo N. Oliveira Jr. [a,*]

[a] Instituto de Física de São Carlos, USP, C.P. 369, 13560-250 São Carlos/SP, Brazil
[b] Departamento de Ciências Exatas e da Terra, Universidade Federal de São Paulo, 09972-270, Diadema, SP, Brazil.
[c] KSV Instruments Ltda, Hötläämötie 7, 00380, Helsinki, Finland

ARTICLE INFO

Article history:
Received 20 December 2009
Accepted 26 February 2010
Available online 3 March 2010

Keywords:
Azopolymers
Optical storage
ATRP
Langmuir–Blodgett
PM-IRRAS

ABSTRACT

The applicability of azopolymers in optical storage can be extended through the use of nanostructured films produced with the Langmuir–Blodgett (LB) technique, but the film properties need to be optimized since these polymers generally do not form stable Langmuir films to be transferred onto solid substrates. Here, photoinduced birefringence was investigated for mixed Langmuir–Blodgett films from the homopolymers 4-[*N*-ethyl-*N*-(2-methacryloxyethyl)]-4′-nitroazobenzene (HPDR1-MA) and poly(dodecylmethacrylate) (HPDod-MA). The interactions between these polymers were studied in Langmuir and LB films. Surface pressure–area isotherms pointed to molecular-level interactions for proportions of 51 mf%, 41 mf% and 31 mf% of HPDR1-MA. Phase segregation was not apparent in the BAM images, in which the morphology of the blend film was clearly different from that of the Langmuir films of neat homopolymers. Through PM-IRRAS, we noted that the interaction between the azopolymer and HPDod-MA affected the orientation of carbonyl groups. Strong interactions for the mixture with 41 mf% of poly(dodecylmethacrylate) led to stable Langmuir films that were transferred onto solid supports as LB films. The photoinduced birefringence of 101-layer mixed LB films show features that make these films useful for optical storage, with the advantage of short writing times in comparison to other azopolymer films.

1. Introduction

Nonlinear optical materials have been widely studied for applications in transmission and manipulation of information, telecommunications, optical signal processing and optical storage [1]. Azopolymers, in particular, have been exploited owing to the properties arising from photoisomerization of the azo groups, especially the photoinduced anisotropy with polarized light [2,3]. The photoisomerization mechanism consists in the reorientation of the azobenzene groups through *trans–cis–trans* isomerization cycles, which produce an excess of chromophores oriented perpendicularly to the laser polarization direction [4,5]. This photoisomerization is highly sensitive to the molecular environment and may be inhibited by aggregation owing to intermolecular interactions. Its kinetics depends on whether the azobenzenes are chemically bonded onto the polymer backbones [6]. Photo-orientation depends on several factors, such as the free volume for the chromophores and the spacer between the azo groups, the main chain structure of the polymer [7–10], the light intensity, and the film thickness [11,12].

The formation of thin films is required for several applications. In this context, highly organized, oriented films can be produced with the Langmuir–Blodgett (LB) technique [10,13], particularly when advantage can be taken of molecular engineering approaches. The latter may be important to obtain stable Langmuir films amenable to transfer onto solid supports, as is the case of mixtures of polymers and amphiphiles. However, such mixed systems are seldom homogeneous, displaying phase separation of the components in the Langmuir and LB films [14–17]. Because phase segregation normally affects other film properties, several combinations of polymers have been used in Langmuir films [18], where the miscibility of the components is inferred from the area per repeating unit at a fixed surface pressure as a function of composition [19]. The expansion or contraction of a mixed monolayer can be related to the Gibbs free energy, in which $\Delta G < 0$ indicates contraction of the mixed monolayer and $\Delta G > 0$ corresponds to monolayer expansion [20].

This paper addresses the molecular-level interactions of a binary mixture containing the azopolymer 4-[*N*-ethyl-*N*-(2-methacryloxyethyl)]-4′-nitroazobenzene (HPDR1-MA) and polydodecylmethacrylate (HPDod-MA) in Langmuir films, for which use was

* Corresponding author.
E-mail address: chu@ifsc.usp.br (O.N. Oliveira Jr.).

0021-9797/$ - see front matter © 2010 Elsevier Inc. All rights reserved.
doi:10.1016/j.jcis.2010.02.061

made of surface pressure and surface potential measurements, in addition to Brewster angle microscopy (BAM) and polarization-modulated infrared reflection absorption spectroscopy (PM-IRRAS). Langmuir–Blodgett (LB) films were then transferred from the mixed monolayers, which could be employed for optical storage.

2. Materials and methods

2.1. Materials and characterization

HPDR1-MA was synthesized via atom transfer radical polymerization (ATRP) using the 4-(*N*-ethyl-*N*-(2-methacryloxyethyl)-4′-nitroazobenzene (DR1-MA) monomer [21] which was obtained by esterification reaction of methacrylic acid and the commercial dye DR1. This polymerization was performed using purified DR1-MA (2.4×10^{-4} mol), ethyl-2-bromobutyrate (EBB) (Aldrich) (6.15×10^{-5} mol) as an initiator, and the catalytic system CuCl/1,1,4,7,10,10 hexamethyltriethylenetetramine (HMTETA) (J.T. Baker/Aldrich) (6.15×10^{-5} mol), for 72 h at 45 °C. HPDod-MA was synthesized via conventional radical polymerization from laurylmethacrylate (Aldrich) (0.074 mol, 23 mL), using AIBN (0.074×10^{-3} mol, 0.0121 g) as initiator at 100 °C for 12 h. The molecular structures of the polymers, which are shown in Scheme 1, were confirmed by their UV–Vis, FTIR and H-NMR spectra, obtained respectively with a Hitachi U-2001 spectrophotometer, in the 1100–190 nm spectral region, Nicolet Nexus 470 spectrophotometer in the region of 4000–400 cm^{-1} using a NaCl window and Bruker AC (200 MHz) spectrometer using deuterated chloroform ($CDCl_3$) as solvents. The molecular weights of these homopolymers were obtained by high-performance size exclusion chromatography (HPSEC) in tetrahydrofuran (THF) at 35 °C (1 mL/min), using polystyrene standards in an Agilent 1100 chromatographic system, with refraction index detector.

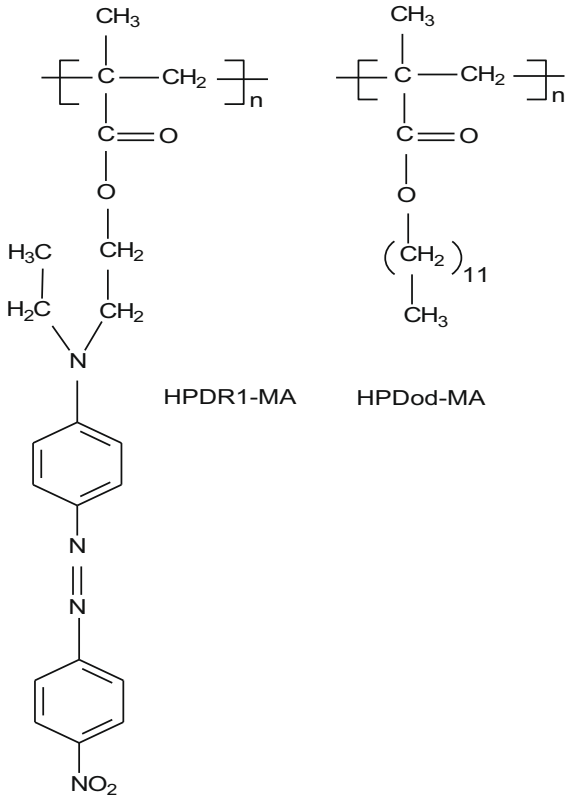

Scheme 1. Chemical structures and abbreviations of the polymers adopted in this paper.

2.2. Fabrication and characterization of Langmuir films

Langmuir films were prepared at ca 23 ± 1 °C using a KSV-5000 LB system placed on an antivibration table in a class 10,000 clean room. Ultrapure water with resistivity 18.2 MΩ cm supplied by a Milli-RO coupled to a Milli-Q purification system from Millipore was used as subphase. The solutions were obtained by dissolving the polymers in chloroform HPLC grade (99.9%) provided by Aldrich at 0.5 mg/mL, which was sufficiently low to allow for polymer spreading, and spread drop by drop on the pure water surface using a microsyringe. For the neat polymers HPDR1-MA and HPDod-MA the amounts spread corresponded to 2.61×10^{-4} and 3.93×10^{-4} mol, respectively. After the evaporation of the solvent, the surface compression started at a barrier speed of 10 mm min^{-1}. The surface pressure (π) was measured using the Wilhelmy method. Monolayer stability was inferred by holding the monolayer at a compressed state (fixed surface pressure) and monitoring the change in mean molecular area with time. The mean molecular area values were calculated based on the molecular weight of the repeating units of HPDR1-MA (382.5 g mol^{-1}) and HPDod-MA (254.0 g mol^{-1}). Surface potential–area (ΔV–A) isotherms were taken in triplicate using a Kelvin probe. The isotherms were obtained for films from neat polymers and blends with 61%, 41% and 23% molar fraction of HPDR1-MA.

Langmuir films of HPDR1-MA, HPDod-MA and of their mixture with 41% molar fraction of HPDR1-MA were analyzed using PM-IRRAS in a KSV PMI 550 instrument (KSV, Biolin Scientific Oy, Helsinki, Finland). The IR beam impinged on the water surface with an incidence angle of 80° being then reflected. Simultaneous measurements of the spectra for the two polarizations were taken by continuous modulation between *s*- and *p*-polarizations, as described in detail by Buffeteau et al. [22]. All spectra were recorded with 6000 scans with resolution of 8 cm^{-1}. To enable the comparison of the main PM-IRRAS features of the mixture with those of the neat polymers, the spectra were taken at a fixed surface pressure of 10 mN m^{-1}. The spectra were treated with the Origin® software to obtain a flat baseline.

The Langmuir film morphology of the neat polymers and of the mixture with 41% molar fraction of HPDR1-MA was studied with a Brewster angle microscope (BAM) BAM2 Plus (Nanofilm Technologies Germany), equipped with a 10× objective, positioned over a Nima trough.

2.3. Langmuir–Blodgett films

Mixed Y-type LB films were deposited onto hydrophilic substrates, B270 glass, with transfer ratios close to 1.0 at a constant surface pressure of 10 mN m^{-1}, using the vertical dipping method. Polarized UV–Vis spectroscopy was applied for the LB film made with the mixture of HPDR1-MA/HPDod-MA in the molar fraction of 41/59, with measurements taken at room temperature with a Hitachi U-2001 spectrophotometer. A polarizer was introduced between the lamp and the sample to obtain the desired polarized UV irradiation. The polarization direction, either parallel or perpendicular, was defined with respect to the dipping direction. The possible film anisotropy was studied for LB films with 5, 11, 15 and 47 layers, and the dichroic ratio ($A_{//}/A_{\perp}$) was calculated, where $A_{//}$ is the absorption in the *s* polarization and $A_{\perp}$ is the absorption in the *p* polarization. To investigate possible orientations of the functional groups on the LB film of the mixture, the FTIR spectra of the LB and cast films in the transmission (on silicon wafer and NaCl window) and reflectance (on glass coated with gold) modes were

recorded on a Nicolet Nexus Fourier Transform Infrared Spectrometer, with a resolution of 4 cm^{-1} in the region of 4000–650 cm^{-1}.

2.4. Optical storage experiments

Optical birefringence was induced in 101-layer mixed LB films using a linearly polarized Ar^+ continuous laser operating at 514 nm (writing beam), with a polarization angle of 45° with respect to the polarization of the probe beam (reading beam). A low power He–Ne laser at 632.8 nm, passing through crossed polarizers and the sample, was employed as probe to measure the induced birefringence in the film. The dynamics of photoinduced birefringence was studied with writing beam powers varying from 0.4 to 3.5 mW. The optically induced birefringence, Δn, was calculated by measuring the probe beam transmission ($T = I/I_0$) using:

$$\Delta n = (\lambda/\pi d)\sin^{-1}\sqrt{T},$$

where λ is the wavelength of the probe beam, d is the film thickness, I_0 is the incident beam intensity and I is the intensity after the second polarizer. The thickness of these films was obtained from surface profile measurements using a Dektak 150 profilometer.

3. Results and discussion

3.1. Polymerization of HPDR1-MA and HPDod-MA

ATRP was successfully used to prepare a methacrylate homopolymer from an azocontaining monomer. The HPSEC data yielded a weight average molecular weight (Mw) of 10,900 g mol^{-1} with a small polydispersity index of 1.2 for HPDR1-MA, which is typical of ATRP polymers [23]. The molecular structure of HPDR1-MA and HPDod-MA was confirmed with the H-NMR spectra. A comparison of the spectra for the DR1-MA monomer and HPDR1-MA showed the similarity for the peaks and the complete disappearance of the vinylic proton signal of the methacrylate group centered at 5.6 and 6.1 ppm owing to the polymerization reaction. ^{1}H-NMR assignments for the HPDod-MA homopolymer were: 0.89 ppm (6H, CH_3), 1.27 ppm (2H, CH_2—CH_3), 1.62 ppm (2H, backbone CH_2), and 1.84 ppm (2H, CH_2—CH_2—O). Table 1 shows the main FTIR bands assigned to the HPDR1-MA and HPDod-MA structures.

3.2. Study of interactions on Langmuir films

The surface pressure isotherm for HPDod-MA in Fig. 1 displays a long plateau at 10.3 mN m^{-1}, which can be attributed to the collapse of the monolayer. In contrast, the HPDR1-MA isotherm exhibits a liquid-condensed phase that withstands surface pressures above 50 mN m^{-1}. The surface pressures for the mixtures are intermediate between those for the neat homopolymers, as expected. Mixed films with more than 77% molar fraction of HPDod-MA have isotherms resembling that of neat HPDod-MA, while the mixtures with less than 49% resemble the HPDR1-MA isotherm. In Langmuir films of polymers, the area per monomer unit is usually

Table 1
Main peaks in the FTIR transmission spectra, in cm^{-1}, for the polymers.

Vibrational groups	HPDR1-MA	HPDod-MA
CH_2 stretching, (symmetric and asymmetric)	2918 and 2850	2924 and 2854
C=O	1736	1731
C=C stretching in benzene rings	1599	–
CH_2 stretching	1461	1467
NO_2 asymmetric and symmetric stretching	1516 and 1338	–
CH_3 stretching	967	967

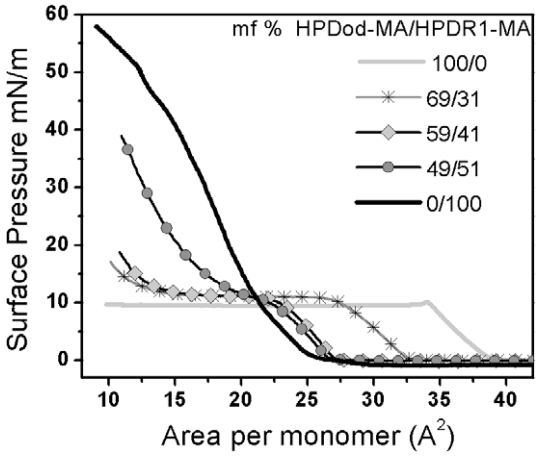

Fig. 1. Surface pressure isotherms for HPDR1-MA, HPDod-MA, and their blends at several proportions.

lower than that expected the monomer would occupy at the interface, owing to possible bending and twisting of the chains, forming a 3D structure. The Langmuir film should not be considered a true monolayer is such cases. Nevertheless, in the experiments reported here the isotherms were reproducible, with negligible influence from the polymer concentration in the solution, and therefore effects from aggregation do not play a major role.

To further examine the interaction between the homopolymers in the films, we plotted in Fig. 2 the changes in Gibbs free energy versus the molar fraction of HPDR1-MA for the surface pressure of 5 mN m^{-1}. ΔG of the HPDR1-MA/HPDod-MA monolayer indicates a strong attraction between the two polymers for the concentrations of 41%, 51% and 61% in molar fraction of HPDR1-MA, which corresponds to the range within which there is considerable increase in the maximum pressure. Similar dependencies were observed for plots made with areas at other fixed surface pressures.

The surface potential isotherms for monolayers of neat HPDR1-MA and HPDod-MA, in addition to mixtures at three relative concentrations, are shown in Fig. 3. These isotherms show a sharp increase in potential at a critical area [24] due to the coming together of domains. This area is usually larger than the onset for the surface pressure isotherm. Also worth noting was the higher surface potential for HPDod-MA. The mixed monolayers displayed intermediate isotherms, normally shifted toward a smaller area in comparison to the isotherm for neat HPDod-MA, as one should expect, since the isotherm for HPDod-MA was also shifted to lower areas. Unfortunately, the isotherms cannot be explained

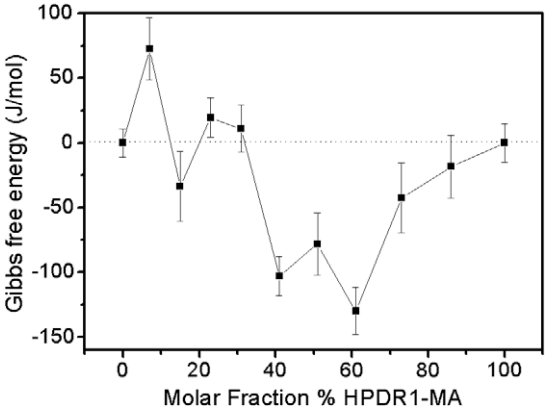

Fig. 2. Plot of mean molecular area at 5 mN m^{-1} versus relative concentration of HPDR1-MA.

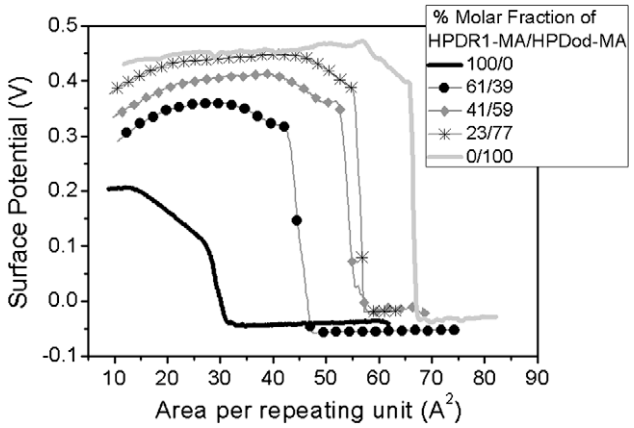

Fig. 3. Surface potential isotherms for monolayers of the homopolymers and mixtures with three relative concentrations of HPDR1-MA and HPDod-MA.

quantitatively because one would need to know the precise positioning of all the polar groups that contribute with large dipole moments to the surface potential. As discussed for other polymers [25], a quantitative interpretation of surface potential measurements is still not possible for macromolecules.

Brewster angle microscopy (BAM) was used to study the morphology of the Langmuir films and possible interactions between the polymers in the mixture [26]. For neat HPDR1-MA, Fig. 4a and d shows that a uniform, homogeneous film is never achieved, though the area occupied by water obviously decreased while the surface pressure increased from 0 (Fig. 4a) to 5 mN m^{-1} (Fig. 4d) leading to the formation of fractures. Even for surface pressures as high as 20 mN m^{-1} (images not shown), the film rigidity prevented the domains formed at lower pressures from coalescing. Fig. 4b and e for HPDod-MA indicate that upon compression the film is relatively uniform, but the whole area of the trough does not seem to be covered. Small domains appear together with black spots that correspond to the subphase water. The mixed Langmuir film displays a morphology that differs from those of the neat homopolymers, as shown in Fig. 4c and 4f for the 1:1 HPDR1-MA:HPDod-MA mixture. In subsidiary experiments we observed that for all mixed films the morphology was different from that of the homopolymers, which may be interpreted as if the mixtures are not made of separate phases of the two polymers. This finding is consistent with the molecular-level interaction suggested to explain the surface pressure and surface potential isotherms of the mixed Langmuir films. The miscibility is also important for the transferability of the Langmuir film onto solid substrates, as we shall discuss later on, for adding HPDod-MA helps the transfer of HPDR1-MA.

The molecular interaction between HPDR1-MA and HPDod-MA was confirmed by polarization-modulated infrared reflection absorption spectroscopy (PM-IRRAS), with Fig. 5 showing that the spectrum for a mixed Langmuir film is not the superimposition of the spectra of the films for the neat polymers. The main feature

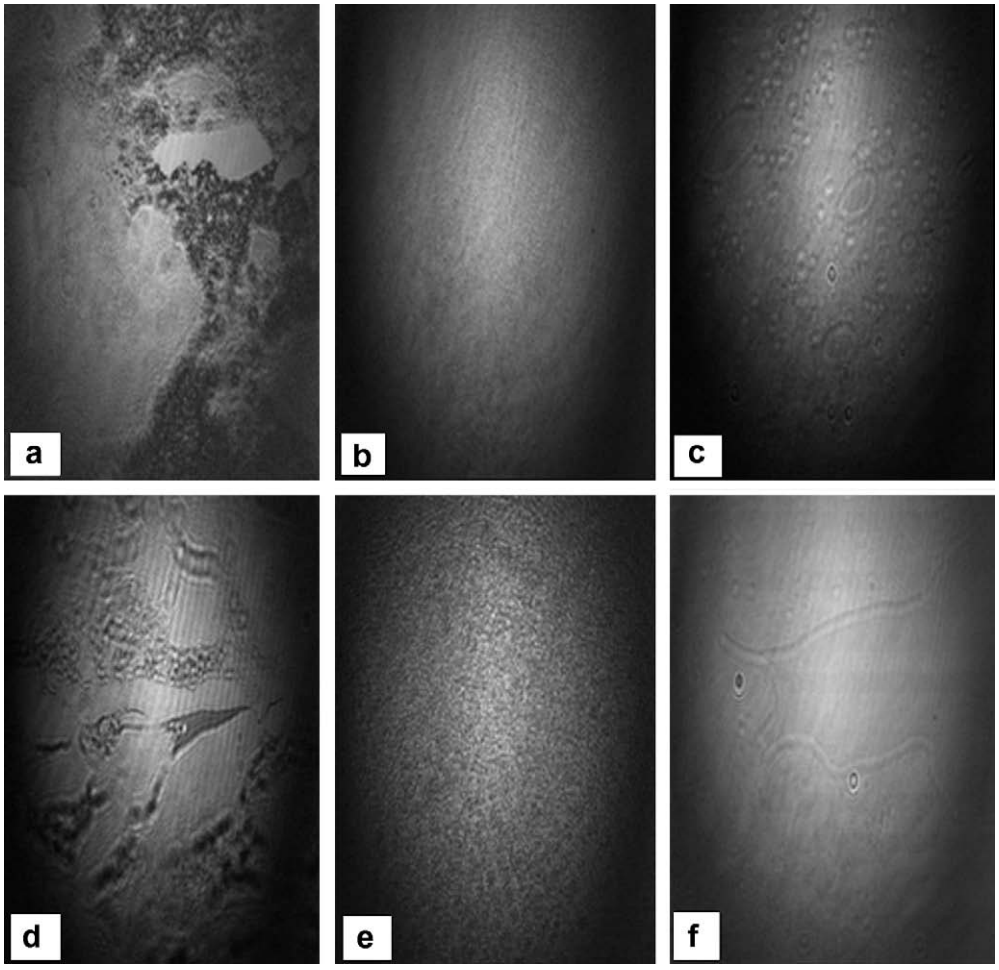

Fig. 4. BAM images (430 × 642 μm^2): from left to right: HPDR1-MA, HPDod-MA and mixture with 41% molar fraction of HPDR1-MA. Top row, $\pi = 0$ and bottom row, $\pi = 5$ mN m^{-1}.

in the PM-IRRAS spectra is the remarkable positive peak at 1730–1745 cm^{-1} corresponding to the ester carbonyl stretching vibration (υ(C=O)), which indicates that most C=O groups have their transition moment oriented perpendicularly to the surface. The shift to lower energies in the band assigned to υ(C=O) is indicative of molecular-level interactions, as this group is sensitive to intra-chain and intermolecular interactions, including those with water molecules at the air–water interface.

For the region between 1050 and 1250 cm^{-1}, corresponding to bands assigned to C—C—O and C—O—C symmetric and asymmetric stretching, the spectrum of the mixed film resembled that of HPDR1-MA. The symmetric and asymmetric stretching bands of CH_2 at 2800–3000 cm^{-1} are not visible in the HPDR1-MA spectrum, due to its lower quantity in the polymer structure, but they are present in the spectra for the films of HPDod-MA and the mixed film. Significantly, a slight shift and broader bands than those of HPDod-MA appear in the spectrum of the mixture, which is a clear confirmation that the spectrum is not a superimposition of the individual spectra for the neat homopolymers.

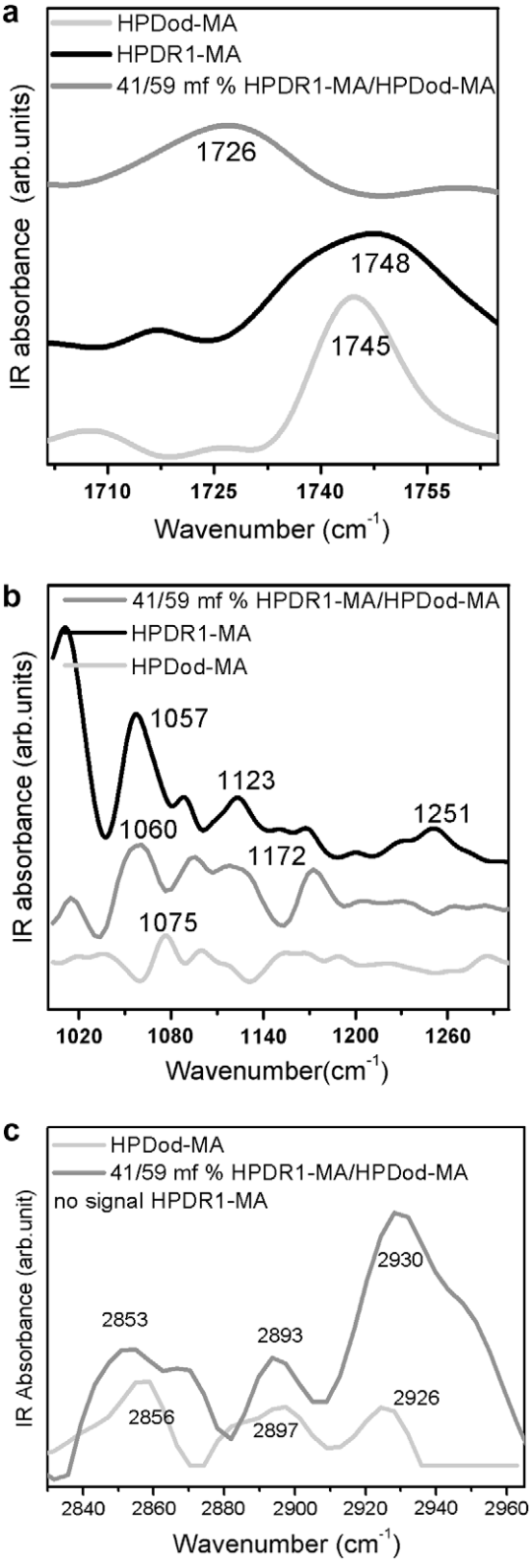

Fig. 5. PM-IRRAS spectra at $\pi = 10$ mN m^{-1} for HPDR1-MA, HPDod-MA, and mixture with 41% molar fraction of HPDR1-MA. (a) At 1700–1770 cm^{-1}, (b) at 1000–1300 cm^{-1} and (c) at 2830–2960 cm^{-1}.

3.3. Langmuir–Blodgett films properties

Films of the pure polymers could not be transferred onto solid substrates with good quality, while the mixed films presented excellent transferability for various substrates, including glass, silicon and gold. The UV–Vis absorption spectrum for the mixed LB film in Fig. 6 exhibits an absorption maximum at 467 nm, ascribed to a π–π^* transition for the azo chromophores. This spectrum is only slightly red shifted in comparison to that of the mixture in chloroform solution, which possesses λ_{max} = 460 nm. Furthermore, the peak in the LB film is not much broader than the peak for the solution (see Fig. 6) as usually seen in LB films. Therefore, such small changes mean that the level of aggregation in these LB films [12,27] is smaller than the usual, probably because HPDod-MA, which does not show significant absorption over the entire UV–Visible range, prevents a strong coupling between the azobenzene groups in the organized LB films.

To investigate possible film anisotropy, polarized UV–Vis absorption spectroscopy experiments were performed. The dichroic ratios ($A_{//}/A_{\perp}$) for the LB films with different numbers of layers at the maximum absorption, assigned to the π–π^* transition of the azobenzene group, ranged from 1.02 to 1.05. The degree of anisotropy is small and therefore the azo groups are almost randomly oriented. The possible orientation of the hydrocarbon chains and other groups cannot be probed with this technique, but this will be addressed with FTIR spectroscopy (see below). The UV–Vis spectroscopy was also useful to monitor the amount of material transferred for distinct numbers of layers in the LB film. Fig. 7a shows the spectra for 41 mf% HPDR1-MA/HPDod-MA LB films with various numbers of layers. The absorbance increased linearly up to

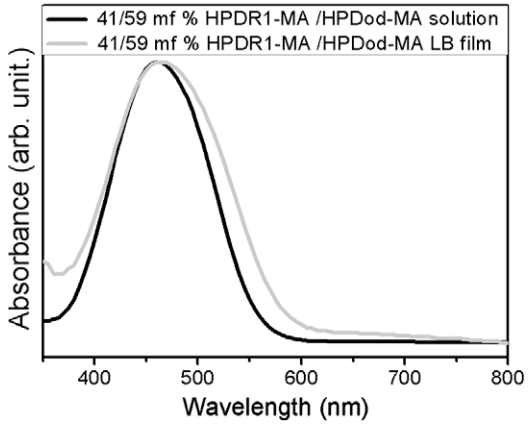

Fig. 6. UV–Vis absorption spectra of 41/59 mf% HPDR1-MA/HPDod-MA in chloroform and in a mixed LB film.

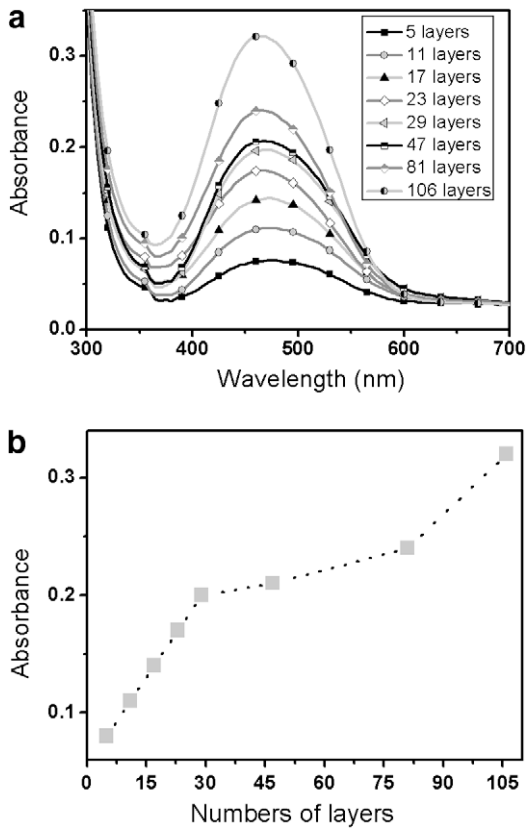

Fig. 7. (a) UV–Vis absorption spectra of LB film of mixture with 41% molar fraction of HPDR1-MA for several numbers of layers. (b) Plot of absorbance at 467 nm versus the number of layers of a mixed LB film.

ca. 30 layers, and then had a smaller slope, as indicated in Fig. 7b. It seems that the transfer of a large number of layers becomes inefficient, which is typical of polymer LB films [28].

Analyzing LB films with FTIR spectroscopy in the absorption and reflection modes may allow one to probe whether the molecules in the film are oriented preferentially and if interactions occur between the polymers. Fig. 8 shows the reflectance and transmittance spectra for 31-layer-LB films of mixture containing 41% molar fraction of HPDR1-MA. The peaks are essentially the same as those in Table 1, which referred to the synthesized polymers. It is worth noting that the transmittance and reflectance spectra for the LB films are quite different. One recalls that the transmittance mode probes vibrations with transition dipole moments in the plane of the film, while vibrations with transition moments normal to the film plane are captured in the reflectance spectra. The absorption bands at 1730 cm^{-1} and 2850–2930 cm^{-1} due to the carbonyl stretching and the CH_2 stretching vibrations are more intense than the aromatic C=C stretching at 1599 cm^{-1} in the reflectance spectrum. Therefore, these groups are preferentially oriented perpendicularly to the substrate surface. In addition, the NO_2 symmetric stretching at 1341 cm^{-1} is less intense than the C=O stretching in the reflectance spectrum indicating that this group is parallel to the substrate surface. The orientation of the chemical groups in the LB film can be compared to that in the cast film, by concentrating on the relative intensity of the C=O and CH_2 stretching vibrations for the reflectance FTIR spectra of the LB and cast films. As Fig. 8 shows, the C=O groups are more strongly oriented perpendicularly to the substrate than in the cast film, which is consistent with the order expected for the LB film.

With regard to the molecular-level interactions between the two polymers, in the spectrum of the mixed LB film one should expected shifts related the interactions observed in the Langmuir films with PM-IRRAS and probable formation of hydrogen bonds in neighboring layers [29]. However, Fig. 8 shows that the spectrum for the LB film is similar to that for the mixed cast film, being a superimposition of the spectra of cast films of the neat polymers (spectra not shown). Therefore, even though some of the order associated with the orientation of C=O groups was preserved in the LB film, the transfer onto the solid substrate hindered the changes that should be caused by other molecular-level interactions between the polymers. This is probably because of the large number of layers required for a good signal-to-noise ratio to be obtained, for which it is known that the order decreases.

3.4. Photoinduced birefringence

Fig. 9 shows the photoinduced birefringence curves for LB films of two mixtures with different azo contents, for the lower

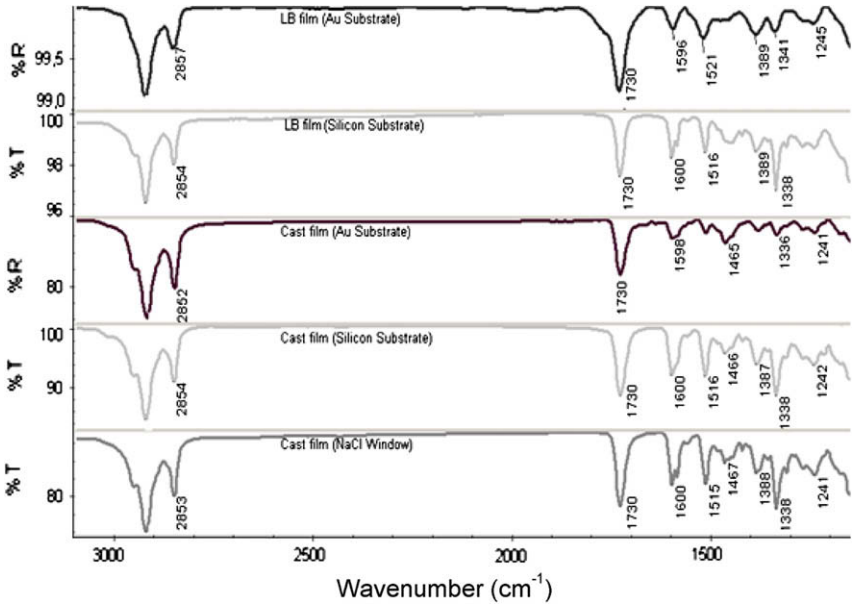

Fig. 8. Reflectance and transmittance FTIR spectra for 31-layer-LB and cast films containing 41/59 mf% HPDR1-MA/HPDod-MA.

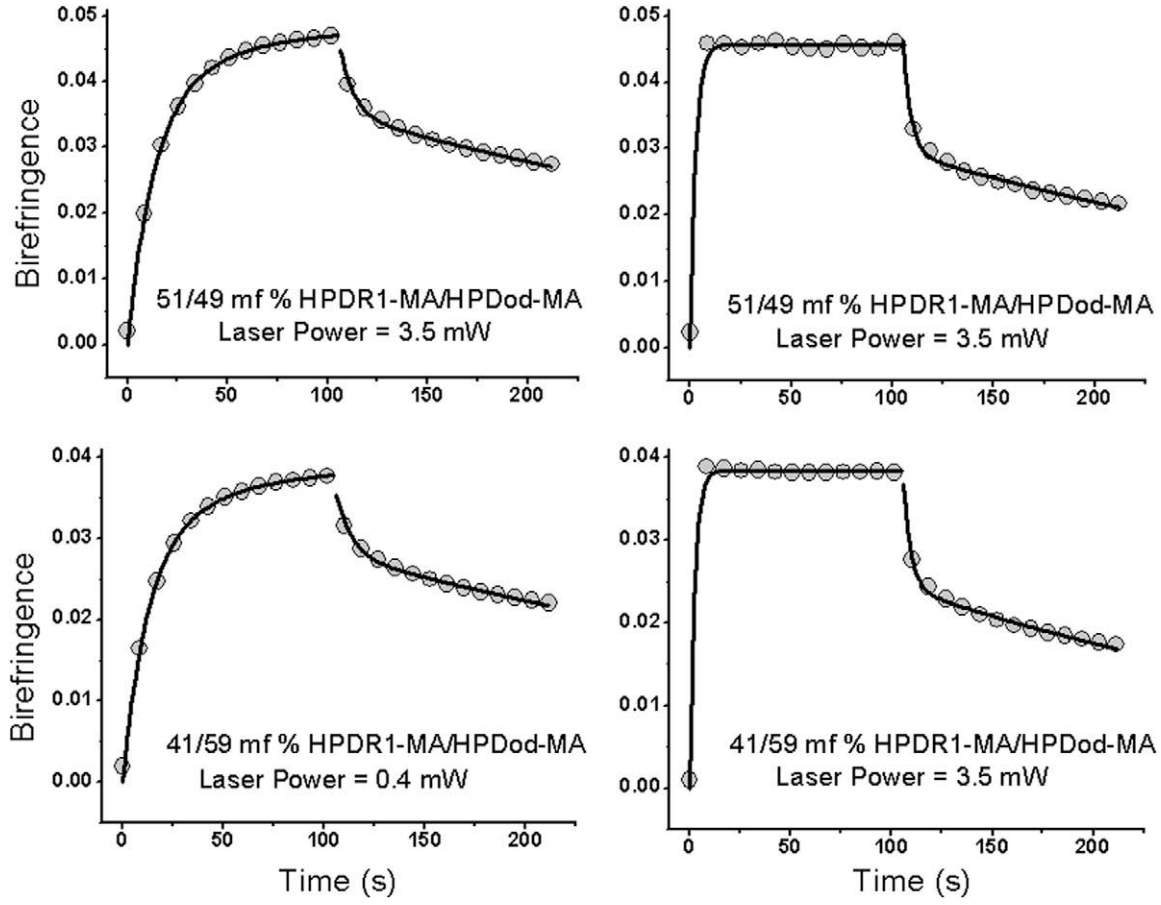

Fig. 9. Buildup and decay of the photoinduced birefringence for a 101-layer-LB film containing 51/49 mf% HPDR1-MA/HPDod-MA at 0.4 mW and 3.5 mW. The solid lines in this figure represent the fitting obtained with Eqs. (1) and (2).

(0.4 mW) and higher (3.5 mW) laser powers used. The dynamics of the photoinduced birefringence comprises two processes: the fast, initial process is attributed to the alignment of azochromophores, while the second, slower process is ascribed to the orientation of chain segments along with the azo moieties. After the writing laser has been switched off, birefringence is lost due to the thermal relaxation of the induced orientation, which can again be modeled with two relaxation processes. The films for the two mixtures display essentially the same behavior, with only a small difference of 0.1 in the birefringence value. The curves for the buildup and decay of birefringence were fitted with biexponential functions of the form

$$\Delta n_{\text{Buildup}} = A_1(1 - e^{-t/\tau_1}) + A_2(1 - e^{-t/\tau_2}) \quad (1)$$

$$\Delta n_{\text{Decay}} = A_3 e^{-t/\tau_3} + A_4 e^{-t/\tau_4} + A_5 \quad (2)$$

where A_1, A_2, A_3, A_4 and A_5 are the pre-exponential factors, t is the time and τ_1, τ_2, τ_3 and τ_4 are the time constants for the fast and slow writing and relaxation processes, respectively. The coefficient A_1 depends on the quantum yield and local mobility of the azo moieties, which is controlled by the size of the azo moieties, the free volume around them and the strength of the coupling interactions between the azo moieties and the polymer backbones. The coefficient A_2 depends on the coupling interaction between the azo moieties and the polymer segments, and on the mobility of the polymer segments. A_3 and A_4 are coefficients representing the fast and slow relaxation processes, with A_3 being attributed to the thermal *cis–trans* isomerization and dipole reorientation while A_4 accounts for the reorientation of chromophores arising from the thermal relaxation of the polymer chains. A_5 represents the fraction of the induced birefringence which is stable over time, i.e., it does not depend on time [30–32].

Table 2 summarizes the parameters used to fit the dynamics of writing and relaxation for the two LB films for a writing power of 0.4 mW. The values of A_1, which corresponds to the fast process of writing, are higher for the film with 51% molar fraction of HPDR1-MA in the mixture, because of the larger number of azochromophores. The time constants τ_1 and τ_2, however, did not change with the number of azo units in the mixture. For this low

Table 2
Parameters obtained by fitting the birefringence curves in Fig. 9 with Eqs. (1) and (2) for the lower laser power, 0.4 mW. We kept the parameters with several decimal places, just for the sake of numerical calculations.

mf% HPDR1-MA	Buildup				Decay				
	$\tau_1(s)$	$\tau_2(s)$	A_1	A_2	$\tau_3(s)$	$\tau_4(s)$	A_3	A_4	A_5
51	13.00	45.70	0.036	0.011	3.84	55.79	0.082	7.715	0.025
41	12.02	48.81	0.010	0.028	3.45	55.51	0.083	18.717	0.024

Table 3
Parameters obtained by fitting the birefringence curves of the mixtures with Eqs. (1) and (2) at different laser powers.

mf% HPDR1-MA	Laser Power (mW)	Buildup		Decay				
		$\tau_1(s)$	A_1	$\tau_3(s)$	$\tau_4(s)$	A_3	A_4	A_5
51	1.4	5.473	0.028	2.24	49.20	0.130	4.325	5.473
51	2.6	2.807	0.022	2.73	50.56	0.093	7.003	2.807
51	3.5	2.771	0.024	2.23	52.76	0.085	5.342	2.771
41	1.4	4.221	0.018	3.74	65.16	0.077	2.394	0.018
41	2.6	3.141	0.018	3.79	59.74	0.067	1.395	0.020
41	3.5	2.482	0.019	2.88	52.04	0.078	9.020	0.017

laser power (0.4 mW), we clearly observed two distinct time constants, with τ_2 being 3.5 times τ_1. For the higher power (3.5 mW), however, τ_2 and τ_1 were identical, thus pointing to a photoinduced orientation determined only by a fast process, attributed to the local movement of the azobenzenes groups in the *trans–cis–trans* isomerization. Thus, one single exponential function may represent the photoisomerization buildup process, as illustrated in Table 3. The values of τ_1 show that a relatively high storage speed can be reached for the mixtures at 3.5 mW.

When the writing beam was switched off, two relaxation processes were apparent. The initial, fast decay occurred with a time constant close to 3 s while the second process, associated with the mobility and relaxation of the polymer backbone, was much slower with a characteristic time constant close to 55 s. The presence of two relaxation processes was observed regardless of the laser power used to photoinduce the birefringence. The fitting with the biexponential function for the decay indicated similar relaxation rates for the two mixtures, as shown in Tables 2 and 3. Note that we kept the values of characteristic times and other parameters in the tables with several decimal places for the sake of the numerical calculations. From the measurements we cannot obviously identify the characteristic times with such accuracy. The presence of the low T_g polymer, HPDod-MA, in the mixture could lead to a faster decay of dipole orientation. However, with the azo chromophores being attached as side groups in the polymer backbone and with the close packing of the LB films, the relaxation processes were slow. The compensation of competing effects is also related to the restrictions in the chromophores mobility in an LB film, which affect both the photoisomerization efficiency and the kinetics of writing and decay. For example when chromophores are closely packed into an ordered structure such as LB films, photoisomerization is hampered because of the lack of free volume [33,34]. The A_5 values correspond to the birefringence kept after long times, which will be discussed below in the analysis of the residual birefringence.

We investigated the effect of varying the laser power on the optically induced birefringence for LB films (thicknesses of approximately 170 nm) with 41% and 51% molar fraction of HPDR1-MA. The amplitude of the birefringence increased slightly with the contents of azochromophores in the sample, being independent of the power of the writing beam within the experimental error (result not shown). In addition, one could infer that a laser power of 0.4 mW was sufficient to induce birefringence in a 101 layer-LB film for any proportion, with $\Delta n = 0.038$ and 0.047 for the mixtures with 41% and 51% molar fraction of HPDR1-MA, respectively. The saturation was reached at the power of 1.4 mW for the two mixtures analyzed.

A desirable characteristic for optical storage systems is short writing and reading times. The time to achieve 50% of the maximum birefringence ($T_{50\%}$) decreased drastically as the laser power was increased from 0.4 to 1.4 mW, as seen in Fig. 10a. Upon further increasing the laser power (up to 3.5 mW), only small changes were noted in $T_{50\%}$. $T_{50\%}$ was independent of the azo content in the mixture, with similar values for mixtures with 41% and 51% molar fraction of HPDR1-MA, as indicated in Fig. 10a. The use of a polymer with low T_g mixed with the azopolymer facilitates the *trans–cis* isomerization leading to a fast rate of achieving the birefringence close to 3 s for the laser power of 1.4 mW.

Another important requirement for optical storage is the residual birefringence after the writing laser is switched off. The mixed LB films studied here had a significant number of molecules with the orientation preserved, i.e., the birefringence could be maintained resulting in a considerable residual ratio (RR). Fig. 10b shows that the LB films of the two mixtures exhibited residual ratios between 45% and 58% after 100 s. The A_5 values in Tables 2 and 3 were higher for the mixture containing 51% molar fraction of HPDR1-MA, but this may be attributed to a higher Δn that increases with the contents of azochromophores. The calculated residual birefringence ratios were similar for the two mixtures. While the structural polymer characteristics such as chain mobility or chain entanglement affect the residual birefringence, the RR values obtained are a consequence of the freedom to move found by chromophores in the mixture. Close to 50% of the birefringence signal lost did so in a very short time, because of the mobility in the mixed film afforded by the presence of HPDod-MA, whose T_g is ca. −65 °C. Our results show that by increasing the laser power five times a decrease in the RR value of 10% was observed, as indicated in Fig. 10.

In summary, the LB films with the HPDR1-MA/HPDod-MA mixtures displayed a residual birefringence that makes them applicable in optical storage. The features of the photoinduced birefringence are similar to analogous systems with azopolymers

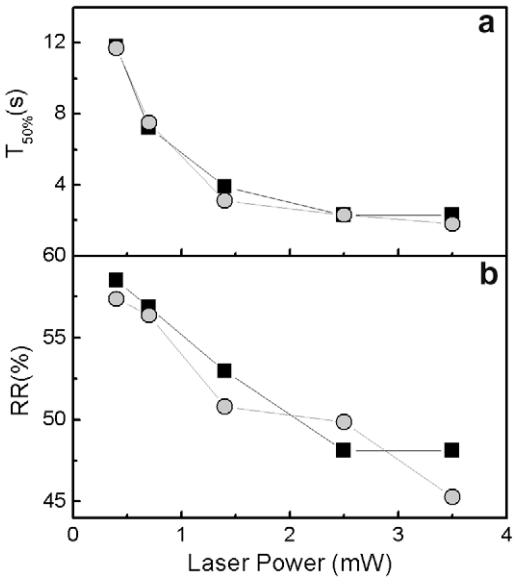

Fig. 10. Dependence of birefringence properties with the laser power for mixed 101-layer-LB films with 51% (square) and 41% (circle) of HPDR1-MA, $T_{50\%}$ (a) and residual birefringence (RR) (b). The lines are drawn to guide the eye.

[4,10,24,35], copolymers [5,10,17,36,37] and blends [38,39] with the advantage of a relatively small writing time. The comparison of the two mixtures indicated that 41% molar fraction of azopolymer are sufficient for the photoinduced birefringence, with an optimized writing process using 1.4 mW of laser power.

4. Summary

The surface pressure isotherms pointed to an interaction between HPDR1-MA and HPDod-MA for proportions from 31% to 61% fraction molar of HPDR1-MA. By examining the isotherms, it was possible to conclude that the mixtures containing 31–41% fraction molar of HPDR1-MA are the most adequate for deposition of Langmuir–Blodgett films. For the mixture containing 41% molar fraction of HPDR1-MA, the PM-IRRAS spectra indicated strong molecular interaction with a shift in the peak assigned to C=O and CH_2 vibration stretching. Furthermore, BAM images showed no phase separation of the polymers, again attributed to a molecular-level interaction. Good quality LB films could not be obtained from pure HPDR1-MA monolayers due to the rigidity of film. In contrast, uniform LB films with several numbers of layers were obtained with the aid of the polymethacrylate HPDod-MA. The UV–Vis results indicated that the presence of HPDod-MA prevented aggregation of the azo chromophores. In polarized UV–Vis absorption spectroscopy, the azo side chains in the polymer films were shown to have no preferred orientation, while the FTIR spectra in reflectance and transmittance mode showed changes on the molecular orientation in the LB films.

The LB films of the HPDR1-MA/HPDod-MA mixtures were amenable to achieve a photoinduced birefringence, with relatively small writing times for a sufficiently high laser power. Other features of these films, including maximum birefringence and residual ratio, demonstrate that these mixtures are promising for use in optical storage, with the possible tuning of the properties by varying the relative concentrations of the mixtures.

Acknowledgments

This work had the financial support from Capes, FAPESP and CNPq (Brazil).

References

[1] X. Chen, J. Zhang, H. Zhang, Z. Jiang, G. Shi, Y. Li, Y. Song, Dyes Pigm. 77 (2008) 223.
[2] A. Natansohn, P. Rochon, Chem. Rev. 102 (2002) 4139.
[3] S.K. Yesodha, C.K.S. Pillai, N. Tsutsumi, Prog. Polym. Sci. 29 (2004) 45.
[4] C. Cojocariu, P. Rochon, J. Mater. Chem. 14 (2004) 2909.
[5] H. Takase, A. Natansohn, P. Rochon, J. Polym. Sci., Part B: Polym. Phys. 39 (2001) 1686.
[6] R. Fernandez, I. Mondragon, M.J. Galante, P.A. Oyanguren, J. Polym. Sci., Part B: Polym. Phys. 47 (2009) 1004.
[7] G. Iftime, L. Fisher, A. Natansohn, P. Rochon, Can. J. Chem. 78 (2000) 409.
[8] R. Fernandez, I. Mondragon, M.J. Galante, P.A. Oyanguren, Eur. Polym. J. 45 (2009) 788.
[9] A. Natansohn, P. Rochon, M.S. Ho, C. Barrett, Macromolecules 28 (1995) 4179.
[10] S. Gimeno, P. Forcen, L. Oriol, M. Pinol, C. Sanchez, F.J. Rodriguez, R. Alcala, K. Jankova, S. Hvilsted, Eur. Polym. J. 45 (2009) 262.
[11] P. Rochon, D. Bissonnette, A. Natansohn, A.S. Xie, Appl. Opt. 32 (1993) 7277.
[12] O.N. Oliveira Jr., D.S. dos Santos, D.T. Balogh, V. Zucolotto, C.R. Mendonça, Adv. Colloid Interface Sci. 116 (2005) 179.
[13] C.R. Mendonça, A. Dhanabalan, D.T. Balogh, L. Misoguti, D.S. Santos, M.A.P. Silva, J.A. Giacometti, S.C. Zilio, O.N. Oliveira Jr., Macromolecules 32 (1999) 1493.
[14] S. Dante, V. Erokhin, L. Feigin, F. Rustichelli, Thin Solid Films 210 (1992) 637.
[15] L.F. Chi, M. Anders, H. Fuchs, R.R. Johnston, H. Ringsdorf, Science 259 (1993) 213.
[16] L.F. Chi, H. Fuchs, R.R. Johnston, H. Ringsdorf, Thin Solid Films 242 (1994) 151.
[17] X. Xu, M. Era, T. Tsutsui, S. Saito, Thin Solid Films 178 (1989) 541.
[18] T.H. Chou, Y.S. Lin, W.T. Li, C.H. Chang, J. Colloid Interface Sci. 321 (2008) 384.
[19] V.R. Shembekar, A. Dhanabalan, S.S. Talwar, A.Q. Contractor, Thin Solid Films 342 (1999) 270.
[20] A.A. Hidalgo, A.S. Pimentel, M. Tabak, O.N. Oliveira Jr., J. Phys. Chem. B 110 (2006) 19637.
[21] F.J. Pavinatto, J.Y. Barletta, R.C. Sanfelice, M.R. Cardoso, D.T. Balogh, C.R. Mendonça, O.N. Oliveira Jr., Polymer 50 (2009) 491.
[22] T. Buffeteau, B. Desbat, J.M. Turlet, Appl. Spectrosc. 45 (1991) 380.
[23] T.E. Patten, K. Matyjaszewski, Adv. Mater. 10 (1998) 910.
[24] O.N. Oliveira Jr., C. Bonardi, Langmuir 13 (1997) 5920.
[25] A. Dhanabalan, R.B. Dabke, N.P. Kumar, S.S. Talwar, S. Major, R. Lal, A.Q. Contractor, Langmuir 13 (1997) 4395.
[26] K. Inglot, T. Martynski, D. Bauman, Opto-Electron. Rev. 17 (2009) 120.
[27] Z.H. Tang, M.S. Johal, P. Scudder, N. Caculitan, R.J. Magya, S. Tretak, H.L. Wang, Thin Solid Films 516 (2007) 58.
[28] A. Dhanabalan, A. Riul Jr., L.H.C. Mattoso, O.N. Oliveira Jr., Langmuir 13 (1997) 4882.
[29] M. Haro, J. Del Barrio, A. Villares, L. Oriol, P. Cea, M.C. Lopez, Langmuir 24 (2008) 10196.
[30] X. Meng, A. Natansohn, C. Barrett, P. Rochon, Macromolecules 29 (1996) 946.
[31] M.S. Ho, A. Natansohn, P. Rochon, Macromolecules 28 (1995) 6124.
[32] M. Jin, Q.X. Yang, R. Lu, L.Y. Pan, P.C. Xue, Y. Zhao, Opt. Mater. 24 (2003) 445.
[33] M. Haro, B. Giner, I. Gascon, F.M. Royo, M.C. Lopez, Macromolecules 40 (2007) 2058.
[34] H. Tachibana, R. Azumi, M. Tanaka, M. Matsumoto, S. Sako, H. Sakai, M. Abe, Y. Kondo, N. Yoshino, Thin Solid Films 284 (1996) 73.
[35] M.S. Ho, C. Barrett, J. Paterson, M. Esteghamatian, A. Natansohn, P. Rochon, Macromolecules 29 (1996) 4613.
[36] M. Jin, R. Lu, Q.X. Yang, C.Y. Bao, R. Sheng, T.H. Xu, Y. Zhao, J. Polym. Sci., Part A: Polym. Chem. 15 (2007) 3460.
[37] L.L. Carvalho, T.F.C. Borges, M.R. Cardoso, C.R. Mendonça, D.T. Balogh, Eur. Polym. J. 42 (2006) 2589.
[38] A. Natansohn, P. Rochon, C. Barrett, A. Hay, Chem. Mater. 7 (1995) 1612.
[39] L.F. Ceridório, M.R. Cardoso, F.J. Pavinatto, A.J.F. Carvalho, C.R. Mendonça, D.T. Balogh, Polym. Int. 55 (2006) 1069.